Study on the sensitivity of optical cavity length to light power fluctuation

Wen Qi (祁 文), Yanyi Jiang (蒋燕义)*, Xueyan Li (李雪艳), Li Jin (金 丽), Zhiyi Bi (毕志毅), and Longsheng Ma (马龙生)

State Key Laboratory of Precision Spectroscopy, East China Normal University, Shanghai 200062, China
**Corresponding author: yyjiang@phy.ecnu.edu.cn*

Received May 9, 2016; accepted August 5, 2016; posted online August 30, 2016

The length stability of optical cavities is vital in ultra-stable, cavity-stabilized laser systems. Using finite element analysis, we study the length deviation of optical cavities due to thermal expansion and thermo-refractive effects when the incident light power is changed. The simulated fractional length sensitivity of a 7.75-cm-long football cavity to the power fluctuation of incident light is $5 \times 10^{-14}/\mu W$, which is in agreement with the experimental results found by measuring the frequency change of a cavity-stabilized laser when the incident light power is changed. Based on the simulation, the cavity sensitivity to light power fluctuation is found to depend on the cavity size and material.

OCIS codes: 140.3425, 140.4780, 120.2230.
doi: 10.3788/COL201614.101401.

Ultra-stable narrow-linewidth lasers are essential in many applications, such as the optical atomic clock, high-resolution laser spectroscopy, tests of fundamental physics, and gravitational wave detection[1–3]. Most of those lasers are achieved by actively stabilizing the laser frequency to the resonance of a Fabry–Perot (F-P) cavity using the Pound-Drever-Hall (PDH) technique[4]. State-of-the-art laser systems have been developed with a linewidth below 1 Hz and fractional frequency instabilities at the 10^{-16} level or better at a 1 s averaging time[5–8].

In those cavity-stabilized laser systems, the laser frequency stability is mostly limited by the length stability of the reference cavities. A special design of optical cavities as well as their supporting configurations has been performed to achieve a low sensitivity to thermal fluctuation and vibration[8–10], approaching a thermal-noise-limited performance[11].

In a cavity-stabilized laser system, the power of light incident onto a cavity is stabilized since the power fluctuation of cavity resonant light induces temperature fluctuation and thus the cavity length fluctuation is due to thermal expansion (TE) and the thermo-refractive (TR) effect. Fractional power instability of 1×10^{-4} can be achieved after stabilization[12]. Usually, the power-dependent frequency shift of a cavity-stabilized laser is measured to be a few tens of hertz/microwatt (Hz/μW)[12], corresponding to a cavity length sensitivity at the 10^{-14} m/μW level. For a 10-cm-long cavity made of ultra-low expansion (ULE) glass, the light power fluctuation-induced fractional length instability is nearly 10^{-16}, while the thermal-noise-limited length instability of the cavity at room temperature is approximately 8×10^{-16}. In the pursuit of a laser frequency instability of 10^{-17} level or better, it is critical to reduce the cavity length instability resulting from light power fluctuation. In this Letter, we study the sensitivity of the cavity length to light power fluctuation (S), providing a method to evaluate the sensitivity S for cavity-stabilized laser systems, as well as providing a way to reduce S by designing an optical cavity with a particular size and material.

We use finite element analysis (FEA) to analyze the length deviation of an F-P cavity when the power of incident light varies. A portion of incident light is absorbed by mirror coatings, resulting in a temperature change. By performing a thermal-mechanical analysis, the displacement between the cavity mirrors due to TE (ΔL_{TE}) is obtained. Meanwhile, the effective optical length change due to the TR effect (ΔL_{TR}) is considered into the total cavity length change by evaluating the temperature variation based on thermal analysis. The length sensitivity of a 7.75-cm-long football cavity to the power fluctuation of incident light is simulated to be $S = 5 \times 10^{-14}/\mu W$. It is in agreement with the experimental results, which are obtained by measuring the frequency change of a cavity-stabilized laser when the cavity incident light power is changed. Based on the FEA, we find that a long cavity made of materials with high thermal conductivity and a small coefficient of TE (CTE) has a low sensitivity S.

Consider an F-P cavity with two highly reflective mirrors optically contacted to a spacer. To achieve a reflectivity of 99.99%, the mirror substrates are usually covered by dielectric coatings, such as multiple layers of SiO_2 and Ta_2O_5. Usually the coatings have a CTE of at the 10^{-5}/K level. Compared with mirror substrates and a cavity spacer that made of fused silica (FS) or ULE glass whose CTE is on the order of 1×10^{-7}/K or less, the deformation of the coatings is unneglectable. Therefore, mirror coatings must be taken into account in the simulation. However, we simplify the N alternating sequences of quarter-wavelength layers into one layer with thickness (d), an averaging density (ρ), Young's modulus (E), and Poisson's ratio (σ), which are listed in Table 1.

Table 1. Main Parameters Used in the Numerical Calculations

Material	ULE[a]	FS[a][13]	Silicon[b][7,14–16]	Sapphire[c][14,17,18]	SiO_2/Ta_2O_5[a][13,14,19]	SiO_2/Ta_2O_5[d][14,20]	GaAs/$Al_{0.92}Ga_{0.08}As$[a][21,22]
E (GPa)	67.6	72	187.5	464	72/140	60/140	100
σ	0.17	0.17	0.28	0.23	0.17/0.23	0.159/0.21	0.32
ρ (kg/m^3)	2210	2200	2330	3997	2200/6850	2200/6850	4551
α (/K)	2×10^{-10}[†]	5.5×10^{-7}	1.7×10^{-9}/ 4.6×10^{-13}[#]	8.8×10^{-11}	5.1×10^{-7}/ -4.4×10^{-5}	-2.5×10^{-7}/ 5.8×10^{-7}	5.7×10^{-6}/ 5.2×10^{-6}
κ (W/m/K)	1.31	1.38	500/10[#]	110	1.38/33	0.13/0.07	62.9[§]
C (J/kg/K)	767	670	0.22	0.09	746/306	1/3.17	360[§]
ε	0.85	0.85	0.55	0.47	N.A	N.A	N.A

[a]at 300 K.
[b]at 124 K.
[c]at 5 K.
[d]at 10 K.
[†]estimated value.
[#]at 1.6 K.
[§]effective value of the coating.

According to Refs. [19,22], the effective CTE (α), capacity (C), and thermal conductivity (κ) of the coating with N layers each of thickness d_j are

$$\alpha_c^{\text{eff}} = \sum_{j=1}^{N} \alpha_j \frac{d_j}{d} \frac{1+\sigma_s}{1-\sigma_j} \left[\frac{1+\sigma_j}{1+\sigma_s} + (1-2\sigma_s) \frac{E_j}{E_s} \right], \quad (1)$$

$$C_c^{\text{eff}} = \sum_{j=1}^{N} C_j \frac{d_j}{d}, \quad (2)$$

$$\kappa_c^{\text{eff}} = \left(\sum_{j=1}^{N} \frac{1}{\kappa_j} \frac{d_j}{d} \right)^{-1}, \quad (3)$$

where the subscripts j, s, and c stand for the coating layer j, the substrate, and the coating. The number of layer pairs of dielectric mirror coating for a reflectivity of 99.995% is typically $N = 19$, while the number for a crystalline coating is typically $N = 40.5$[21]. For the dielectric coating at room temperature, $C_c^{\text{eff}} = 566\ \text{J} \cdot (\text{kg} \cdot \text{K})^{-1}$, and $\kappa_c^{\text{eff}} = 2.27\ \text{W} \cdot (\text{m} \cdot \text{K})^{-1}$, while at the cryogenic, $C_c^{\text{eff}} = 2\ \text{J} \cdot (\text{kg} \cdot \text{K})^{-1}$, and $\kappa_c^{\text{eff}} = 0.1\ \text{W} \cdot (\text{m} \cdot \text{K})^{-1}$. The α_c^{eff} used throughout this Letter are listed in Table 2.

When a single frequency laser light is on resonance of a F-P cavity, the total loss is

$$P_l = P_{in} - P_r - P_t, \quad (4)$$

where P_{in}, P_r, and P_t are the cavity input and the reflected and transmitted light power. Since the input laser light is phase modulated for frequency stabilization[4], we assume the modulation index is nearly one, and thus 60% of P_{in} remains in the carrier and couples into the cavity, while the sidebands are nearly reflected from the cavity. Usually 90% of the light can be coupled to the TEM_{00} mode of the cavity, and what is left is coupled to higher order modes. Moreover, we assume the ratio of mirror absorption to scattering is about 1:4[22]. Hence each mirror absorbs a total power of $0.054 \times P_l$.

In the simulation, on each mirror, a heat flow of $0.054 \times P_l$ is applied to an area in the coating center. We apply a step function (six steps within $1.52 \times \omega_0$, where ω_0 is the light beam radius) to simulate the Gaussian distribution of the light power, as shown in Fig. 1(a). The error due to the non-Gaussian distribution of the light power is within 5%. To obtain a steady solution, thermal radiation to the surroundings is imposed at the outside surface of the cavity with thermal emissivity (ε). The emissivity of the surroundings is assumed to be 0.1 for all the following simulations. Taking advantage of the geometrical symmetry of the cavities, the nodes in the symmetrical plane of the cavity are constrained within the symmetrical plane. A thermal-mechanical analysis is performed to investigate the distance displacement between the probe points along the cavity's optical axis, and a thermal analysis is performed to obtain the temperature change of the probe points when the incident light power changes. The probe

Table 2. Calculated Effective CTEs for Coatings

Substrate	Coating	α_c^{eff} (/K)	β_c^{eff} (/K)
ULE	SiO_2/Ta_2O_5	-6.5×10^{-5}	-1.4×10^{-5}
FS	SiO_2/Ta_2O_5	-6.3×10^{-5}	-1.4×10^{-5}
Silicon[*]	SiO_2/Ta_2O_5	2.6×10^{-7}	2.7×10^{-6}
Sapphire[†]	SiO_2/Ta_2O_5	2.1×10^{-7}	2.7×10^{-6}
FS	GaAs/$Al_{0.92}Ga_{0.08}As$	1.9×10^{-5}	7.9×10^{-5}

[*]at 124 and 1.6 K.
[†]at 5 K.

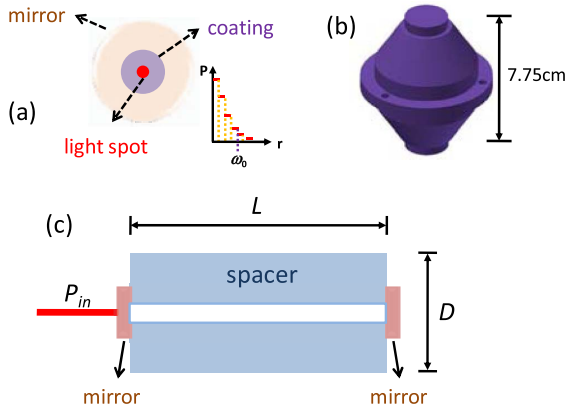

Fig. 1. (a) Diagram of a high-reflective mirror. It is coated at the center with a diameter of 10 mm. The red spot at the coating center represents a light spot to which an absorbed light power is applied. Schematic diagram of (b) a football cavity and (c) a cylinder cavity.

points are distributed within ω_0. The cavity length change is obtained by averaging those probe points.

We use this method to simulate the sensitivity S of our football cavity and compare it with the measurement.

The cavity structure is symmetrically wider in the middle and tapered at the ends, as shown in Fig. 1(b). The cavity spacer is 7.75-cm-long, and two mirrors are optically connected to the cavity spacer. Both the cavity spacer and the mirror substrates are made of ULE glass. The mirrors are coated with high-reflective films of SiO_2 and Ta_2O_5 at 1064 nm.

Experimentally, we measured the sensitivity S by monitoring the frequency change of the beat note between two cavity-stabilized laser systems when the incident light power of one cavity was changed. The experimental diagram is shown in Fig. 2. Using the PDH technique, the frequency of each laser is stabilized to the resonance of its cavity by feeding back the error signal to a piezo transducer (PZT) for frequency adjustment. When the incident light power of Laser #1 was changed from 6.5 to 8.5 μW, the frequency change of the beat note monitored by a counter with a gate time of 1 s is 50 Hz, as shown in the inset of Fig. 2. It takes about 2 s for the cavity length to resettle to the new input light power. At the time of ~130 s, the incident light power of Laser #1 was changed back to 6.5 μW in order to cancel the residual drift of the cavity resonant frequencies on the measurement. The sensitivity S of this cavity to the power change of the incident light is measured to be 8.8×10^{-14}/μW.

We measured the cavity loss by measuring P_r and P_t to be 11.7 and 3.7 μW, accordingly, on the photo detectors (PD_1 and PD_2) when light with power $P_{in} = 17.7$ μW is incident and on resonance of the cavity. Thus, the fractional loss of the cavity is $13\% \times P_{in}$.

In the simulation, $d = 6$ μm, and $\omega_0 = 250$ μm. When P_{in} is changed from 6.5 to 8.5 μW, the cavity deforms due to the change of light power absorption. Figure 3(a) shows the cavity deformations due to TE. As we can see, only the points where heat flow is applied have an observable displacement. By averaging the probe points within ω_0, $\Delta L_{\mathrm{TE}} = 7.9 \times 10^{-15}$ m. It is worth noting that in the simulation ΔL_{TE} includes the deformation of both cavity spacer and mirrors, while in the measurement the deformation of the cavity spacer is not measured since it takes a few hours for the cavity spacer to heat up and expand due to its large mass. By simulation, we calculated the length change of the cavity spacer to be on the order of 1×10^{-17} m, which is negligible.

For another, when P_{in} is changed from 6.5 to 8.5 μW, the temperature of the coating also changed accordingly, which is $\Delta T = 6$ μK based on the steady-static thermal analysis of the FEA. Figure 3(b) shows the temperature change of the probe points inside ω_0 (blue open squares) based on the transient thermal analysis. It takes 2 s for the cavity to almost adjust to the new incident light power, which agrees with the temporal behavior shown in the inset of Fig. 2. On the contrary, it takes a longer time for the probe points on the mirror contacting surface of the cavity spacer due to its bigger mass.

The effective TR coefficient of the coating is[22]

$$\beta_c^{\mathrm{eff}} = \frac{B_H + B_L}{4(n_H^2 - n_L^2)}, \tag{5}$$

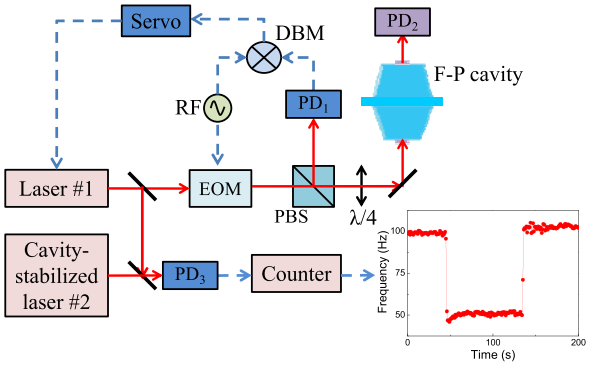

Fig. 2. Experimental setup for the measurement of the cavity sensitivity S. EOM, electro-optic modulator; PBS, polarization beam splitter; λ/4, quarter-wave plate; PD, photo detector; RF, radio frequency; DBM, double balance mixer.

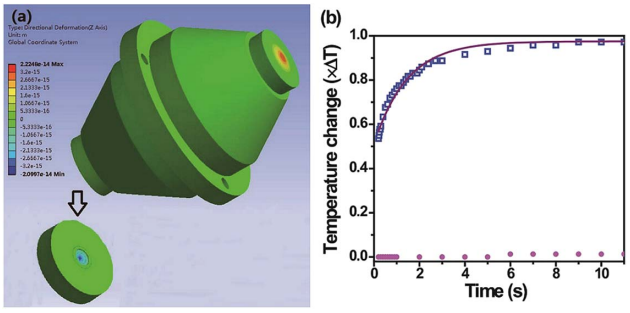

Fig. 3. (a) The thermally induced deformations of the cavity. (b) The temperature change of the probe points inside ω_0 (blue open squares) and those on the mirror contacting surface (pink dots) over time.

where $B_x = \beta_x + \alpha_x n_x(1+\sigma_x)/(1-\sigma_x)$ and subscript $x = H$, L stands for the high and low index material of the coating. β_x and n_x are the coefficients of thermo-refraction and index of the coating layer x. The β_c^{eff} of various coatings on different substrates are listed in Table 2. Therefore,

$$\Delta L_{\text{TR}} = -2\beta_c^{\text{eff}} \lambda \times \Delta T, \tag{6}$$

where λ is the light wavelength. For the football cavity, $\Delta L_{\text{TR}} = 6 \times 10^{-17}$ m, which is two orders of magnitude smaller than ΔL_{TE}.

As a result, the total cavity length change is $\Delta L = 7.9 \times 10^{-15}$ m, corresponding to a fractional cavity length sensitivity $S = \Delta L/(L \times \Delta P_{in}) = 5 \times 10^{-14}/\mu\text{W}$. The discrepancy between the measurement and the simulation may arise from an inaccurate estimate of the mirror absorption loss and the CTE of the coating. For example, if the mirror absorption loss equals the mirror scattering, the sensitivity S will be $1.3 \times 10^{-13}/\mu\text{W}$.

Next, we study the sensitivity S by varying the cavity size and material when P_{in} changes from 10 to 11 μW. To simplify the cavity structure, in the following simulations the cavity is in the shape of a cylinder with a length of $L = 10$ cm, a diameter of $D = 10$ cm, and an axial hole of 10 mm for light access, as shown in Fig. 1(c). Two mirrors with a diameter of 25.4 mm and a thickness of 6.35 mm, made of ULE glass and coated with SiO_2/Ta_2O_5, are bonded to the ULE spacer. $P_l = 13\% \times P_{in}$, $d = 6$ μm, and $\omega_0 = 250$ μm. For this cavity, S_0 is simulated to be $3.2 \times 10^{-14}/\mu\text{W}$. Then, the cavity size, CTE, Young's modulus, thermal conductivity, and Poisson's ratio of the cavity (including spacer and mirror substrate) and coating double separately. Based on the FEA, we obtain S in each case, where ΔL_{TR} is also much smaller than ΔL_{TE}. Figure 4(a) shows the relative sensitivity S/S_0.

The sensitivity S is inversely proportional to L. Since the deformations of the cavity mirrors are almost the same, while increasing L, the fractional length and S reduces accordingly. The sensitivity S has a relatively weak correlation to D.

The CTE of the mirror coating has a great effect on S. S nearly doubles as α_c^{eff} changes from -6.5×10^{-5} to -1.3×10^{-4}/K. Therefore, it is important to use accurate CTE values of the coating. However, to date the CTE of Ta_2O_5 varies, i.e., 3.6×10^{-6} or -4.4×10^{-5}/K[14,15], and its CTE at a cryogenic temperature was deduced to be 5.8×10^{-7}/K by only one group[20]. The uncertainty of the coating CTE gives the biggest contribution to the simulation error. On the contrary, the CTE of the cavity has less of an effect on S. However, S increases nonlinearly when increasing the CTE of the cavity, as shown with blue open triangles in Fig. 4(b). Interestingly, S reduces when increasing E of the cavity, while it increases when increasing that of the coating. This situation happens when changing σ. It is due to the negative α_c^{eff}. The thermal conductivity of the cavity also has a great effect on S, while that of the coatings has little effect on S. However, when κ of the cavity spacer and mirror substrate is larger than 50, S is less sensitive to it, as shown with black filled triangles in Fig. 4(b). When increasing κ, the temperature becomes more uniform, which makes less strain inside the cavity and coating, resulting in less of a change of the cavity length.

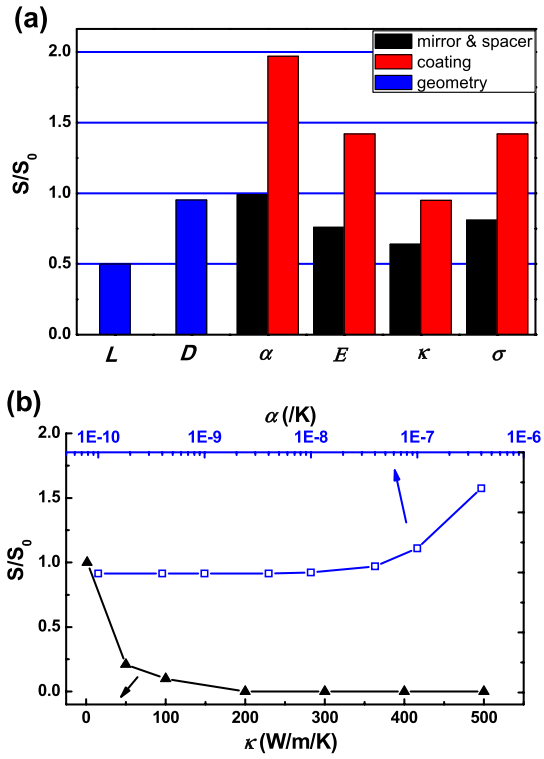

Fig. 4. Simulation results of S/S_0 (a) when the parameters of the cavity and coating are doubled and (b) when the CTE (blue open squares, upper axis) or the thermal conductivity (black filled triangles, lower axis) of the cavity and mirror substrate changes.

Next, we change the materials of the cavity, mirror substrate, and coating to explore the sensitivity S based on the FEA. The simulation results are listed in Table 3. The FS and ULE are usually used in room temperature cavities. While reducing the temperature of the cavities for less thermal noise, silicon and sapphire are employed since they have a relatively small CTE at low temperatures[7,17,23,24]. The crystalline coating of $GaAs/Al_{0.92}Ga_{0.08}As$ is also used for lower cavity thermal noise due to its lower mechanical loss compared to the dielectric coating of SiO_2/Ta_2O_5[21,22]. In the table, the corresponding fractional cavity length instabilities are listed when the incident light power is 10 μW with a fractional instability of 1×10^{-4}.

As we can see in the table, for a dielectric coating at room temperature, ΔL_{TR} is much smaller than ΔL_{TE}. The sensitivity of an all-ULE cavity is smaller than that of an all-FS cavity since the CTE of ULE is three orders of magnitude smaller than that of FS. The sensitivity of a cavity with a ULE spacer and FS mirror substrates is about the same as that of an all-ULE cavity. The sensitivity S of the silicon cavity at 1.6 K is $1 \times 10^{-17}/\mu\text{W}$, about the same as that at 124 K due to the smaller κ and CTE.

Table 3. Simulated Sensitivity S when the Cavity Material Varies[a]

Spacer	Mirror	Coating	ΔL_{TE} (m)	ΔL_{TR} (m)	S (/μW)	$\Delta L/L$ (10^{-18})
FS	FS	SiO_2/Ta_2O_5	5.7×10^{-15}	7×10^{-17}	5.8×10^{-14}	58
ULE	ULE	SiO_2/Ta_2O_5	3.1×10^{-15}	7×10^{-17}	3.2×10^{-14}	32
ULE	FS	SiO_2/Ta_2O_5	3.4×10^{-15}	7×10^{-17}	3.5×10^{-14}	35
ULE	FS	$GaAs/Al_{0.92}Ga_{0.08}As$	4.0×10^{-16}	2×10^{-16}	6×10^{-15}	6
Silicon	Silicon	SiO_2/Ta_2O_5	$6\times10^{-18}{}^{*}/8\times10^{-18}{}^{\#}$	2×10^{-18}	$8\times10^{-18}{}^{*}/1\times10^{-17}{}^{\#}$	$0.008^{*}/0.01^{\#}$
Sapphire	Sapphire	SiO_2/Ta_2O_5	$3\times10^{-18}{}^{\dagger}$	$2\times10^{-18}{}^{\dagger}$	$5\times10^{-18}{}^{\dagger}$	$0.005^{\dagger}$

[a]The cavity has a length of 10 cm and a diameter of 10 cm. $\Delta L/L$ is the fractional cavity length instability when light with a power of 10 μW and a power instability of 1×10^{-4} is incident onto and on resonance of the cavity.
[*]at 124 K.
[#]at 1.6 K.
[†]at 5 K.

For a 25-cm-long silicon cavity at 1.6 K, the sensitivity S is measured to be 3×10^{-14}/μW in Ref. [15], while in our simulation for the same cavity, it is 4×10^{-18}/μW. The biggest difference may arise from the CTE value of Ta_2O_5 at a cryogenic temperature. If we assume the CTE of Ta_2O_5 at 1.6 K is -2×10^{-4}/K, the simulated sensitivity of the silicon cavity agrees with the measured result. The sensitivity for the sapphire cavity at 5 K is slightly smaller than the silicon cavity at 1.6 K due to its bigger E and κ. When the dielectric coating is replaced with the crystalline coating of $GaAs/Al_{0.92}Ga_{0.08}As$, the sensitivity S is reduced to 6×10^{-15}/μW, which results from the smaller α_c^{eff} and bigger κ of the crystalline coating.

In this Letter, we use FEA to simulate the sensitivity of cavity length to light power fluctuation. The simulated sensitivity of a 7.75-cm-long football cavity is 5×10^{-14}/μW, which is in agreement with the experimental results. Based on the simulation, a cavity with a longer length is found to have less sensitivity. When the cavity is made of materials with higher thermal conductivity and Young's modulus or a smaller CTE and Poisson's ratio, it is less sensitive to light power fluctuation.

This work was supported by the National Natural Science Foundation of China (Nos. 11374102 and 11334002) and the Shanghai Rising-star Program (No. 15QA1401900).

References

1. A. D. Ludlow, M. M. Boyd, J. Ye, E. Peik, and P. O. Schmidt, Rev. Mod. Phys. **87**, 637 (2015).
2. X. Fu, K. Liu, R. Zhao, W. Gou, J. Sun, Z. Xu, and Y. Wang, Chin. Opt. Lett. **13**, 073001 (2015).
3. C. H. Eisele, A. Y. Nevsky, and S. Schiller, Phys. Rev. Lett. **103**, 090401 (2009).
4. R. W. P. Drever, J. L. Hall, F. V. Kowalski, J. Hough, G. M. Ford, A. J. Munley, and H. Ward, Appl. Phys. B **31**, 97 (1983).
5. B. C. Young, F. C. Cruz, W. M. Itano, and J. C. Bergquist, Phys. Rev. Lett. **82**, 3799 (1999).
6. Y. Y. Jiang, A. D. Ludlow, N. D. Lemke, R. W. Fox, J. A. Sherman, L.-S. Ma, and C. W. Oates, Nat. Photon. **5**, 158 (2011).
7. T. Kessler, C. Hagemann, C. Grebing, T. Legero, U. Sterr, F. Riehle, M. J. Martin, L. Chen, and J. Ye, Nat. Photon. **6**, 687 (2012).
8. S. Häfner, S. Falke, C. Grebing, S. Vogt, T. Legero, M. Merimaa, C. Lisdat, and U. Sterr, Opt. Lett. **40**, 2112 (2015).
9. L. Chen, J. L. Hall, J. Ye, T. Yang, E. Zang, and T. Li, Phys. Rev. A **74**, 053801 (2006).
10. X. Dai, Y. Jiang, C. Hang, Z. Bi, and L. Ma, Opt. Express **23**, 5134 (2015).
11. K. Numata, A. Kemery, and J. Camp, Phys. Rev. Lett. **93**, 250602 (2004).
12. Y. Jiang, S. Fang, Z. Bi, X. Xu, and L. Ma, Appl. Phys. B **98**, 61 (2010).
13. V. B. Braginsky and S. P. Vyatchanin, Phys. Lett. A **312**, 244 (2003).
14. J. Franc, N. Morgado, R. Flaminio, R. Nawrodt, I. Martin, L. Cunningham, A. Cumming, S. Rowan, and J. Hough, "Mirror thermal noise in laser interferometer gravitational wave detectors operating at room and cryogenic temperature," http://arxiv.org/abs/0912.0107 (2009).
15. E. Wiens, Q.-F. Chen, I. Ernsting, H. Luckmann, U. Rosowski, A. Nevsky, and S. Schiller, Opt. Lett. **39**, 3242 (2014).
16. N. M. Ravindra, B. Sopori, O. H. Gokce, S. X. Cheng, A. Shenoy, L. Jin, S. Abedrabbo, W. Chen, and Y. Zhang, Int. J. Thermophys. **22**, 1593 (2001).
17. S. Seel, R. Storz, G. Ruoso, J. Mlynek, and S. Schiller, Phys. Rev. Lett. **78**, 4741 (1997).
18. A. M. Wittenberg, J. Opt. Soc. Am. **55**, 432 (1965).
19. M. Evans, S. Ballmer, M. Fejer, P. Fritschel, G. Harry, and G. Ogin, Phys. Rev. D **78**, 102003 (2008).
20. A. Farsi, M. S. de Cumis, F. Marino, and F. Marin, J. Appl. Phys. **111**, 043101 (2012).
21. G. D. Cole, W. Zhang, M. J. Martin, J. Ye, and M. Aspelmeyer, Nat. Photon. **7**, 644 (2013).
22. T. Chalermsongsak, E. D. Hall, G. D. Cole, D. Follman, F. Seifert, K. Arai, E. K. Gustafson, J. R. Smith, M. Aspelmeyer, and R. X. Adhikari, Metrologia **53**, 860 (2016).
23. M. Cerdonio, L. Conti, A. Heidmann, and M. Pinard, Phys. Rev. D **63**, 082003 (2001).
24. J.-P. Richard and J. J. Hamilton, Rev. Sci. Instrum. **62**, 2375 (1991).